



Cite this: *Chem. Commun.*, 2021, **57**, 1818

Received 16th December 2020,
Accepted 6th January 2021

DOI: 10.1039/d0cc08160d

rsc.li/chemcomm

Substituted *meso*-vinyl-BODIPY as thiol-selective fluorogenic probes for sensing unfolded proteins in the endoplasmic reticulum†

Huiying Mu,^a Koji Miki,^{*a} Takuya Kubo,^{id}^b Koji Otsuka^{id}^b and Kouichi Ohe^{id}^{*a}

A new type of thiol probes based on the *meso*-vinyl-BODIPY (VB) scaffold were developed. The monochloro-substituted VB1Cl exhibited the largest fluorescence enhancement (>200-fold) as well as high selectivity upon biological thiol sensing. VB1Cl was successfully applied for reporting the protein unfolding process under ER stress in living cells.

Biological thiols including small-molecule thiols, such as glutathione (GSH) and cysteine (Cys), and thiol-containing proteins participate in diverse physiological and pathological processes within a cell.¹ Alterations in the levels of small-molecule thiols and the irreversible overoxidation of Cys on proteins under oxidative stress are known to be associated with many human diseases, such as inflammatory diseases, Alzheimer's disease, and cancers.² Therefore, monitoring cellular thiol levels and selectively labeling protein Cys by fluorescence imaging should provide insight into the molecular mechanisms of the involved physiopathological processes.³

Fluorogenic probes that have an 'off' state and can 'turn-on' fluorescence upon reaction with analytes, are attractive for sensitive detection and high-contrast bioimaging.⁴ Thiol-reactive fluorescent probes have been extensively developed by exploiting diverse chemical reactions, such as thiol-disulfide exchange, maleimide-thiol addition, and thiol alkylation by iodoacetamide.^{3,5} Maleimide-based probes are the most representative examples for thiol-selective bioconjugation and detection.⁶ Keillor *et al.* have reported a series of dimaleimide-based probes which allow fluorogenic labeling of proteins that are genetically fused with a specific peptide tag.⁷ Very recently, Hong *et al.* demonstrated the use of maleimide-functionalized tetraphenylethene (TPE) and its derivatives to sense the protein unfolding process in the endoplasmic reticulum (ER) of

living cells.⁸ Protein folding in the ER is quality controlled by cellular proteostasis.⁹ Failure in proper protein folding can lead to a loss of protein function and the cytotoxic accumulation of unfolded proteins causes ER stress, which is associated with cell apoptosis and neurodegenerative disorders, such as Alzheimer's disease and Parkinson's disease.¹⁰ Fluorogenic TPE derivatives could label the exposed Cys thiols upon protein unfolding, which are buried inside protein structures under the normal conditions. However, the short excitation wavelength (~400 nm) of TPE fluorophore may cause damages on biological specimens after long-term irradiation, and its broad emission (500–750 nm) could be readily overlapped with those of fluorescent markers during the multi-color imaging. Moreover, the maleimide-based probes suffer from common limitations of compromised chemoselectivity to thiols and decreased stability of the maleimide-thiol adduct under relatively basic conditions, especially at pH > 8.¹¹

Herein, we report a new type of thiol-reactive fluorogenic probes, referred to as VBs, derived from *meso*-vinyl-BODIPY (Fig. 1). The electron deficiency of the BODIPY core and the high nucleophilicity of the mercapto group enable the selective and fluorogenic addition reaction of thiols to the vinyl group, in a wide pH range (5–10). After the incorporating of electron-withdrawing groups at the BODIPY core, the monochloro-substituted VB1Cl, is applicable for sensing small-molecule thiols and labeling unfolded proteins with high selectivity and sensitivity. In living cell imaging, VB1Cl exhibited good organelle specificity in lysosomes and the ER. Furthermore, the

^a Department of Energy and Hydrocarbon Chemistry, Graduate School of Engineering, Kyoto University, Katsura, Nishikyo-ku, Kyoto 615-8510, Japan. E-mail: kojimiki@scl.kyoto-u.ac.jp, ohe@scl.kyoto-u.ac.jp

^b Department of Material Chemistry, Graduate School of Engineering, Kyoto University, Katsura, Nishikyo-ku, Kyoto 615-8510, Japan

† Electronic supplementary information (ESI) available: Experimental section, MTT assay, spectroscopic, NMR spectra, and mathematical illustration. CCDC 2034710. For ESI and crystallographic data in CIF or other electronic format see DOI: 10.1039/d0cc08160d

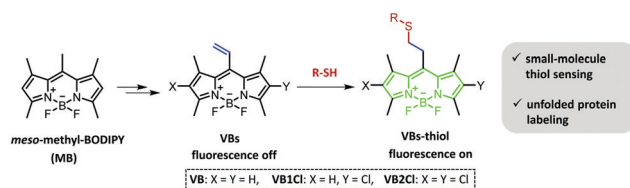


Fig. 1 Substituted *meso*-vinyl BODIPY (VBs) as thiol-selective fluorogenic probes for small-molecule thiol sensing and unfolded proteins labeling, prepared from *meso*-methyl-BODIPY (MB).

potential utility of **VB1Cl** for detecting unfolded proteins under ER stress in living cells was demonstrated.

The vinyl product **VB** was prepared from *meso*-methyl-BODIPY **MB** through a stepwise synthetic route (Scheme S1, ESI†).¹² In an effort to increase the electrophilicity of **VB**, the electron-withdrawing chloro groups were introduced to the pyrrole ring of BODIPY core to yield **VB1Cl** and **VB2Cl**. The structure of **VB1Cl** was further identified by X-ray crystallography (Fig. S1 and Table S1, ESI†). With the probes **VBs** in hand, we then firstly investigated the photophysical properties. **VBs** exhibited extremely weak fluorescence with low fluorescence quantum yield (<0.006) in ethanol (Table S2, ESI†). The absorption and fluorescence maxima of chloro-substituted probes **VB1Cl** and **VB2Cl** were slightly bathochromic shifted compared with **VB**, which is because the substitution with chloride at C2 and C6 position of BODIPY core decrease the HOMO–LUMO energy gap.¹³ Similar with the conventional tetramethyl-BODIPY dyes, **VBs** showed narrow absorption and fluorescence bands, which is ideal for multi-color imaging. The reaction of **VBs** with thiols was examined using a model reaction, in which the non-fluorescent **VB** was transformed to a highly fluorescent adduct through the addition of a thiol to the β -carbon of the *meso*-vinyl group. The structures were confirmed by NMR and HR-MS analyses (Fig. S2, ESI†). We next investigated the response of **VBs** to biological thiols by spectroscopic measurements. Upon the addition of Cys to the solutions of **VB1Cl** and **VB2Cl**, remarkable fluorogenic response was observed over time (Fig. 2a). After 1 h incubation, 232- and 41-fold fluorescence enhancements were detected for **VB1Cl** and **VB2Cl**, respectively, which were much higher than that of **VB** (Fig. S3, ESI†). This result highlighted the increased reactivity of the *meso*-vinyl group upon incorporation of electron-withdrawing groups at the BODIPY core. The more electron-deficient **VB2Cl** weakened the turn-on fluorescence increment due to its relatively high fluorescence background. Therefore, probe **VB1Cl** was selected for further applications.

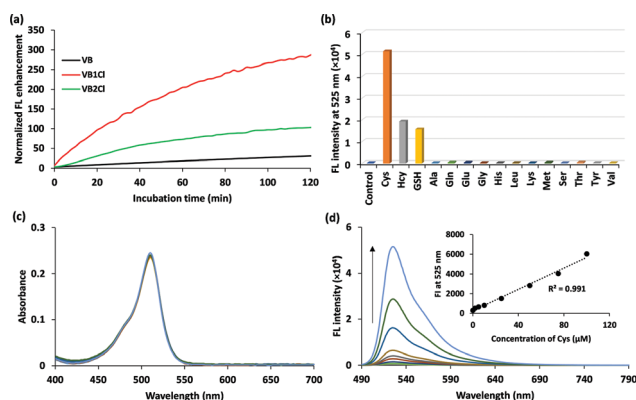


Fig. 2 (a) Time-dependent normalized fluorescence enhancement ($FL_{\text{probe-Cys}}/FL_{\text{probe}}$) of **VBs** in presence or absence of Cys (1 mM) in PBS (pH 7.2, 0.1 M)/MeCN (1/1, v/v). **VB** and **VB1Cl**: at 525 nm; **VB2Cl**: at 543 nm. (b) Selectivity of **VB1Cl** toward a variety of amino acids (1 mM) after 1 h incubation. (c) Absorption and (d) fluorescence spectra of **VB1Cl** upon treatment of Cys (0–1 mM). Inset: Calibration curve of fluorescence intensity at 525 nm vs. Cys (0–100 μ M). Incubation time: 1 h. Dye: 5 μ M. λ_{ex} = 480 nm.

To gain insight into the selectivity of **VB1Cl**, the fluorescence response toward various amino acids was examined (Fig. 2b). Among the amino acids tested, only Cys, GSH, and homocysteine (Hcy), which contain mercapto groups, induced significant changes in the fluorescence of **VB1Cl**, highlighting the probe's high selectivity toward biological thiols over other nucleophiles such as hydroxy and amino groups. Furthermore, the spectroscopic titration of **VB1Cl** toward small-molecule thiols was conducted (Fig. S4–S6, ESI†). Upon the addition of Cys, the fluorescence intensity of **VB1Cl** at 525 nm increased markedly, in a Cys-concentration-dependent manner, with a good linear correlation in the range 0–100 μ M (Fig. 2d), while the absorption spectra remained unchanged (Fig. 2c). The effect of pH on the fluorescence response of **VB1Cl** to amino acids was also investigated (Fig. S7, ESI†). **VB1Cl** displayed good stability and exhibited weak fluorescence in the pH range 5–10, in which the response of **VB1Cl** to Cys could be activated (Fig. S7a, ESI†). It is important to note that **VB1Cl** displayed high chemoselectivity to thiols even under basic conditions at pH 9.8, without any response to lysine up to 24 h (Fig. S7b and c, ESI†). This property is relevant advantage of our **VBs** over the conventional maleimide-based thiol probes.^{11b,14} To evaluate the stability of **VB1Cl** and its thiol-adduct under basic conditions, the **VB1Cl**-GSH adduct was isolated by HPLC (Fig. S8a, ESI†). The time-dependent fluorescence of **VB1Cl** and **VB1Cl**-GSH were measured in a buffer solution at pH 9.8 (Fig. S8b, ESI†). The thiol-adduct remained intact after 24 h incubation, relying on its extremely high stability, which is superior to the maleimide-based probes.¹⁵ The other adducts of **VB1Cl** with the Cys and Hcy were characterized by liquid chromatography-tandem mass spectrometer (LC-MS/MS) and HR-MS (Fig. S9, ESI†). In addition, the molecular conformation of **VB1Cl** and its thiol-adduct was estimated by density functional theory (DFT) calculation (Fig. S10, ESI†). We observed the bending of the dipyrin structure in the excited state, leading to non-irradiative relaxation. In contrast, the thiol-adduct of **VB1Cl** recovered the planar dipyrin and favored the emission transition. These results are in good accordance with the findings of previous studies.^{12a,16}

We then explored the utility of **VB1Cl** for detecting the unfolded proteins by fluorogenic labeling of the exposed Cys residues upon protein unfolding. Initially, β -lactoglobulin LGB,¹⁰ which contains five buried thiols, was used as a model protein (\sim 18 kDa) for the in-tube experiments. After the incubation of **VB1Cl** with LGB for 1 h, negligible fluorescence was observed (Fig. 3a and b). LGB could be denatured by urea in a concentration-dependent manner which was characterized by the decreased signals at 286 and 293 nm in near-UV circular dichroism (CD) spectroscopy (Fig. S11, ESI†).¹⁷ Treatment of unfolded LGB with **VB1Cl** gave bright fluorescence with a maximum 468-fold enhancement. Pretreatment with *N*-ethylmaleimide (NEM), a thiol-quenching reagent, completely suppressed the fluorescence enhancement (Fig. 3a and b). Indications were therefore, that **VB1Cl** could selectively label unfolded proteins through the exposed Cys residues. The covalent conjugation of **VB1Cl** with unfolded LGB was also identified by quadrupole Time-of-Flight LC-MS/MS (Fig. S12, ESI†). Moreover, the

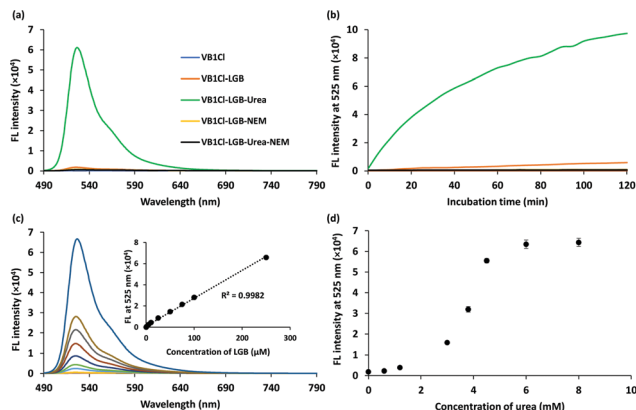


Fig. 3 (a) Fluorescence spectra of **VB1Cl** treated with folded/unfolded LGB for 1 h with/without by NEM (4 mM). Protein denaturant: 6 M urea in PBS (pH 7.2, 0.1 M); LGB: 250 μM . (b) Fluorescence kinetic traces of Fig. 3a. (c) Fluorescence titration of **VB1Cl** with unfolded LGB (0–250 μM). Inset: Calibration curve of fluorescence intensity at 525 nm vs. unfolded LGB. (d) Fluorescence intensity of **VB1Cl** reacted with 250 μM LGB denatured by urea (0–8 M). Dye: 5 μM . $\lambda_{\text{ex}} = 480 \text{ nm}$.

fluorogenic response of **VB1Cl** was linearly correlated with the concentration of the unfolded LGB in the range 0–250 μM (Fig. 3c). In agreement with the CD measurements, the fluorescence of **VB1Cl** was changed in a urea-concentration-dependent manner. The urea concentration for 50% of fluorescence enhancement of **VB1Cl** ($[\text{Urea}]_{1/2} = 4.0 \text{ M}$) was consistent with the reported value ($[\text{Urea}]_{1/2} = 4.3 \text{ M}$) that denatured 50% of LGB molecules (Fig. 3d).^{17a} These results indicate that **VB1Cl** could sensitively detect the degree of protein unfolding by fluorescence output.

The excellent thiol response of **VB1Cl** encouraged us to apply it to living cell systems. The cytotoxicity of **VB1Cl** was first assessed *via* MTT assays (Fig. S14a, ESI[†]). The viability of HeLa cells remained unchanged after incubation with **VB1Cl** (up to 10 μM) for 24 h. Next, living cell imaging was performed with confocal laser scanning microscopy (CLSM). After the incubation of HeLa cells with **VB1Cl** at 37 $^{\circ}\text{C}$ for 1 h, **VB1Cl** penetrated the membranes and stained the cells with bright fluorescence from an emission channel (Fig. 4). When cells were pretreated with NEM before the **VB1Cl** staining, the intracellular fluorescence was substantially reduced. This indicated that the bright fluorescence stems from the selective reaction of **VB1Cl** with endogenous thiols, such as GSH and protein Cys residues. During the course of the cell imaging experiment, we found that **VB1Cl** seemed to have a particular imaging pattern inside cells (Fig. 5). We assumed that the hydrophobic **VB1Cl** ($\text{clog } P = 4.75$) may favor its accumulation in the cellular membrane system. Indeed, **VB1Cl** was moderately colocalized with ER-Tracker Red with a Pearson's correlation coefficient (PCC) value of 0.45 (Fig. 5a). In contrast, the costaining of **VB1Cl** with MitoTracker Deep Red showed a low correlation (PCC = 0.03, Fig. S16, ESI[†]). By staining HeLa cells with **VB1Cl**, punctate signals were also observed at the perinuclear region and they were well merged with LysoTracker Deep Red (PCC = 0.71, Fig. 5b). These results indicated that **VB1Cl** could detect cellular thiols with organelle-specificity in lysosomes and the ER. After the staining of living cells, cold methanol fixation was applied for the precipitation of cellular

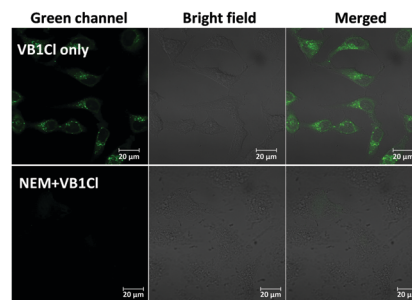


Fig. 4 Confocal fluorescence images of cellular thiols by **VB1Cl** in living HeLa cells. Top: Incubated with **VB1Cl** (5 μM) for 1 h; bottom: pretreated with NEM (2 mM) for 30 min and treated with **VB1Cl** for 1 h. $\lambda_{\text{ex}} = 488 \text{ nm}$, $\lambda_{\text{em}} = 490\text{--}540 \text{ nm}$. Scale bar: 20 μm .

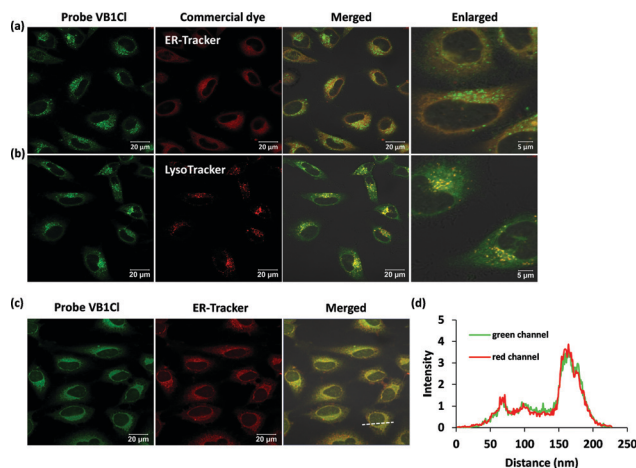


Fig. 5 Representative confocal images of living HeLa cells treated with **VB1Cl** (5 μM) for 1 h and (a) ER-Tracker Red (1 μM) or (b) LysoTracker Deep Red (50 nM) for 15 min. (c) Confocal images of HeLa cells costained with **VB1Cl** (5 μM) and ER-Tracker Red (1 μM), followed by methanol fixation. (d) Fluorescence intensity profiles of two kinds of emissions in the intersted linear region across HeLa cells in the merged figure of (c). Scale bar: 20 μm or 5 μm . Colocalization areas are in yellow. Conditions: for **VB1Cl**, $\lambda_{\text{ex}} = 488 \text{ nm}$, $\lambda_{\text{em}} = 490\text{--}540 \text{ nm}$. For LysoTracker Deep Red, $\lambda_{\text{ex}} = 633 \text{ nm}$, $\lambda_{\text{em}} = 640\text{--}720 \text{ nm}$. For ER-Tracker Red, $\lambda_{\text{ex}} = 561 \text{ nm}$, $\lambda_{\text{em}} = 565\text{--}640 \text{ nm}$.

proteins by removing small molecules. Interestingly, the punctate pattern was significantly diminished while the ER labeling remained and dominated, showing a high colocalization with ER-Tracker Red (PCC = 0.93, Fig. 5c and d). In contrast, control molecule **MB** bearing an unreactive methyl group at the meso position could not label any proteins in cells (Fig. S17, ESI[†]). The results of living cell imaging of organelle-specific **VB1Cl** suggest that detection of the punctate signals is probably due to the reaction with small-molecule thiols, such as GSH and digested proteins, in lysosomes and that proteins should be labeled in the ER through a stable covalent bond.

Relying on the good organelle-specificity of **VB1Cl**, we finally used the probe to monitor the protein unfolding process occurring in the ER of living cells using CLSM imaging (Fig. 6). The ER stress was pharmacologically induced by antibiotic active tunicamycin^{10c,18} and proteasome inhibitor MG132,¹⁹ which can cause an accumulation of unfolded

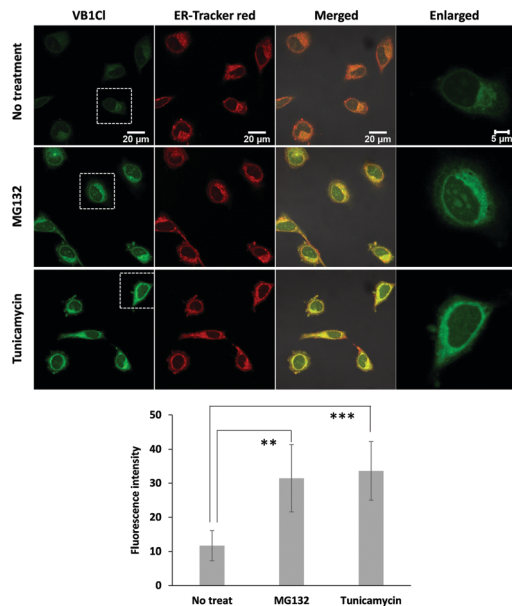


Fig. 6 Confocal images of controlled and stressed HeLa cells stained with **VB1Cl** (5 μ M) for 1 h and ER-Tracker Red (1 μ M) for 15 min, followed by methanol fixation. The white frame showed as enlarged images. Scale bar: 20 μ m or 5 μ m. Colocalization areas are in yellow. The relative fluorescence intensity of green channel from each dish calculated by using image J software. Error bar indicates standard deviation ($n = 5$). Statistical analyses were performed with a *t*-test ($n = 5$) relative to the data of no stress-treated cells. **: <0.05 , ***: <0.001 .

proteins in the ER and inhibit proteasomal degradation of the unfolded proteins, respectively. Compared with the untreated cells, significantly increased fluorescence from the green channel in the ER was observed in the tunicamycin- or MG132-pretreated cells. The results demonstrate that **VB1Cl** indeed has the potential to label unfolded proteins under stimulation conditions that mimic proteostasis imbalance in living cells.

In conclusion, we developed a new type of thiol-reactive fluorogenic probes, **VBs**, derived from *meso*-vinyl-BODIPY. Owing to the electron-deficient nature of the BODIPY core, the vinyl group could react with thiols in a Michael addition manner. The incorporation of chloride further facilitated the addition reaction. The optimized probe **VB1Cl** exhibited a remarkable fluorogenic response (>200 -fold) with small-molecule thiols and unfolded proteins. When coupled with fluorescence microscopy imaging, **VB1Cl** is applicable for detecting cellular thiols with excellent organelle specificity in lysosomes and the ER. Furthermore, the utility of **VB1Cl** for sensitively reporting the protein unfolded process occurring in the ER of living cells under imbalanced proteostasis was demonstrated. Compared with the conventional maleimide-based probes, **VB1Cl** has obvious advantages in chemoselectivity to thiols and stability of the thiol adduct under basic conditions.

This work was supported by a Grant-in-Aid for Scientific Research on Innovative Areas "Middle molecular strategy: creation of higher bio-functional molecules by integrated synthesis (No. 2707)" (18H04404) and Grant-in-Aid for Scientific Research (B) (20H02811). H. M. thanks to a financial support from a Grant-in-aid for JSPS research Fellows (20J15123). K. M. appreciates the financial support from Hoansya Foundation. We acknowledge

Professor Kazuo Tanaka and Assistant Professor Masayuki Gon in Kyoto University for CD measurement.

Conflicts of interest

There are no conflicts to declare.

Notes and references

- (a) Z. Xiao, S. L. Fontaine, A. I. Bush and A. G. Wedd, *J. Mol. Biol.*, 2019, **431**, 158–177; (b) M. Benhar, *Antioxidants*, 2020, **9**, 309; (c) Y. Shi and K. S. Carroll, *Acc. Chem. Res.*, 2020, **53**, 20–31.
- (a) F. Silvagno, A. Vernone and G. P. Pescarmona, *Antioxidants*, 2020, **9**, 624; (b) D. Dwivedi, K. Megha, R. Mishra and P. K. Mandal, *Neurochem. Res.*, 2020, **45**, 1461–1480; (c) E. V. Kalina and L. A. Gavriliuk, *Biochemistry*, 2020, **85**, 895–907; (d) J. Serpa, *Front. Oncol.*, 2020, **10**, 947.
- (a) S. Lee, J. Li, X. Zhou, J. Yin and J. Yoon, *Coord. Chem. Rev.*, 2018, **366**, 29–68; (b) Y. Wang, R. An, Z. Luo and D. Ye, *Chem. – Eur. J.*, 2018, **24**, 5707–5722.
- (a) J. Zhang, X. Chai, X. He, H. Kim, J. Yoon and H. Tian, *Chem. Soc. Rev.*, 2019, **48**, 683–722; (b) E. Kozma and P. Kele, *Org. Biomol. Chem.*, 2019, **17**, 215–233; (c) B. S. McCullough and A. M. Barrios, *Curr. Opin. Chem. Biol.*, 2020, **57**, 34–40.
- (a) L. Niu, Y. Chen, H. Zheng, L. Wu, C. Tung and Q. Yang, *Chem. Soc. Rev.*, 2015, **44**, 6143–6160; (b) C. Yin, K. Xiong, F. Huo, J. C. Salamanca and R. M. Strongin, *Angew. Chem., Int. Ed.*, 2017, **56**, 13188–13198; (c) J. Zhuang, N. Wang, X. Ji, Y. Tao, J. Wang and W. Zhao, *Chem. – Eur. J.*, 2020, **26**, 4172–4192.
- J. M. J. M. Ravasco, H. Faustino, A. Trindade and P. M. P. Gois, *Chem. – Eur. J.*, 2019, **25**, 43–59.
- (a) S. Girouard, M. Houle, A. Grandbois, J. W. Kellor and S. W. Michnick, *J. Am. Chem. Soc.*, 2005, **127**, 559–566; (b) Y. Chen, C. M. Clouthier, K. Tsao, M. Strmiskova, H. Lachance and J. W. Keillor, *Angew. Chem., Int. Ed.*, 2014, **53**, 13785–13788; (c) Y. Chen, K. Tsao, S. L. Acton and J. W. Keillor, *Angew. Chem., Int. Ed.*, 2018, **57**, 12390–12394.
- (a) M. Z. Chen, N. S. Moily, J. L. Bridgford, R. J. Wood, M. Radwan, T. A. Smith, Z. Song, B. Z. Tang, L. Tilley, X. Xu, G. E. Reid, M. A. Pouladi, Y. Hong and D. M. Hatters, *Nat. Commun.*, 2017, **8**, 474; (b) T. C. Owyong, P. Subedi, J. Deng, E. Hinde, J. J. Paxman, J. M. White, W. Chen, B. Heras, W. H. H. Wong and Y. Hong, *Angew. Chem., Int. Ed.*, 2020, **59**, 10129–10135.
- R. Inagi, Y. Ishimoto and M. Nangaku, *Nat. Rev. Nephrol.*, 2014, **10**, 369–378.
- (a) J. Choi and C. Song, *Front. Immunol.*, 2020, **10**, 3147; (b) D. C. Silva, P. Valentao, P. B. Andrade and D. M. Pereira, *Pharmacol. Res.*, 2020, **155**, 104702; (c) C. Hetz, K. Zhang and R. J. Kaufman, *Nat. Rev. Mol. Cell Biol.*, 2020, **21**, 421–438.
- (a) G. T. Hermanson, *The Reactions of Bioconjugation. Bioconjugate Techniques*, Academic Press, NY, 3rd edn, 2013, pp. 229–258; (b) O. Koniev and A. Wagner, *Chem. Soc. Rev.*, 2015, **44**, 5495–5551.
- (a) R. Lincoln, L. E. Greene, C. Bain, J. O. Flores-Rizo, S. S. Bohle and G. Cosa, *J. Phys. Chem. B*, 2015, **119**, 4758–4765; (b) H. Zhu, J. Fan, H. Mu, T. Zhu, Z. Zhang, J. Du and X. Peng, *Sci. Rep.*, 2016, **6**, 35627.
- (a) K. Krumova and G. Cosa, *J. Am. Chem. Soc.*, 2010, **132**, 17560–17569; (b) G. Duran-Sampedro, A. R. Agarrabeitia, I. Garcia-Moreno, A. Costela, J. Banuelos, T. Arbeloa, I. L. Arbeloa, J. L. Chiara and M. J. Ortiz, *Eur. J. Org. Chem.*, 2012, 6335–6350.
- C. F. Brewer and J. P. Riehm, *Anal. Biochem.*, 1967, **18**, 248–255.
- (a) R. P. Liburdy, *J. Phys. Chem.*, 1978, **82**, 870–874; (b) Y. Ishii and S. S. Lehrer, *Biophys. J.*, 1986, **50**, 75–80.
- H. Zhu, J. Fan, M. Li, J. Cao, J. Wang and X. Peng, *Chem. – Eur. J.*, 2014, **20**, 4691–4696.
- (a) D. Galani and R. K. O. Apenten, *Food Res. Int.*, 1999, **32**, 93–100; (b) I. Eberini, C. Sensi, A. Barbiroli, F. Bonomi, S. Iametti, M. Galliano and E. Gianazza, *Amino Acids*, 2012, **42**, 2019–2030.
- (a) N. M. P. Fajardo, C. Meijer and F. A. E. Kruyt, *Biochem. Pharmacol.*, 2016, **118**, 1–8; (b) F. Foufelle and B. Fromenty, *Pharmacol. Res. Perspect.*, 2016, **4**, e00211.
- J. A. Williams, Y. Hou, H. Ni and W. Ding, *Pharm. Res.*, 2013, **30**, 2279–2289.